PAPER

NJC
www.rsc.org/njc

# Aqueous synthesis of group IIIA nitrides at low temperature

**Yujie Xiong,[ab] Yi Xie,*[ab] Zhengquan Li,[b] Xiaoxu Li[b] and Rong Zhang[b]**

[a] *Structure Research Laboratory, University of Science and Technology of China, Hefei, Anhui 230026, P. R. China*
[b] *Department of Chemistry, University of Science and Technology of China, Hefei, Anhui 230026, P. R. China. E-mail: yxielab@ustc.edu.cn; Fax: +86-551-3603987; Tel: +86-551-3603987*

***Received (in Montpellier, France) 27th August 2003, Accepted 1st October 2003***
***First published as an Advance Article on the web 4th December 2003***



Group IIIA nitrides have been synthesized in aqueous solution under mild conditions for the first time. The reaction was carried out in an aqueous solution with $NH_4Cl$ as nitrogen source at 250 °C. X-Ray diffraction, transmission electronic microscope, high-resolution transmission electron microscopy, electronic diffraction patterns, X-ray photoelectron spectra, energy-dispersive X-ray analysis, infrared absorption spectra and ultraviolet and visible light (UV-vis) spectra were used to characterize the products. It was found that the bandgaps of group IIIA nitrides and their alloy nanocrystals can cover the region of 2.1–6.3 eV.

## Introduction

In the past decades, group IIIA nitrides are been the continuing focus of materials synthesis and characterization, owing to their excellent physical properties with large direct energy gaps and potential applications as electronic and optoelectronic materials in the green, blue and ultraviolet spectral regions.[1] Their chemical inertia, resistance to radiation, high thermal conductivities, large avalanche breakdown fields and high-field electron drift velocities[2] have led to their use in high-power applications in caustic environments. Compared to I–VII and II–VI semiconductors, the group IIIA nitride materials have a greater degree of covalent bonding, a less ionic lattice and larger exciton diameters.

In detail, indium nitride (InN) and gallium nitride (GaN) can be used to fabricate laser diodes, *p–n* junctions and full-color, flat-panel displays.[3] Aluminium nitride (AlN) is also currently of great technological importance because of its unique properties such as good electrical resistivity, high thermal conductivity, high mechanical strength and a low thermal expansion coefficient, similar to that of silicon.[4] Their alloys ($Al_xGa_{1-x}N$, $In_xGa_{1-x}N$ and $In_xAl_{1-x}N$) are uniquely suitable for fabricating optoelectronic devices in the ultraviolet-visible bands of the spectrum and as phosphors for large area displays, since their bandgaps can range from 2.0 to 5.9 eV.[5]

Despite the fact that conventional synthetic methods exist, including organometallic precursor routes,[2,6] high pressure direct synthesis,[7] atomic layer epitaxy,[8] reactive magnetron sputtering,[9] chemical vapor deposition (CVD),[10] melt synthesis,[11] halogen-transport vapor phase epitaxy (VPE),[12] microwave heating,[13] thermal metathesis reaction,[14] and molecular beam epitaxy (MBE),[15] a solution-based route is a very attractive alternative for the synthesis of group IIIA nitrides under mild conditions.[16] From the green chemistry point of view, water is an ideal medium for the solution-based route, which has motivated us to explore the possibility of preparing IIIA–V semiconductors in aqueous solution. Recently, our group has successfully prepared GaP and InP nanocrystals *via* reactions between $Ga_2O_3$ or $In_2O_3$ and white phosphorus in aqueous alkali solution.[17] Herein, we present the first aqueous preparation of group IIIA nitrides and their alloy nanocrystals in an acidic system.

## Experimental

In a typical synthesis, 5 mmol $M_2S_3$ (M = In, Ga, Al), 60 mmol $NH_4Cl$, 15 mmol $CS_2$ and 7.5 mmol $I_2$ was added into a 50 ml Teflon-lined autoclave, which was then filled with distilled water up to 80% of the total volume (pH ≈ 6). Argon gas was passed through the solution to drive off the air dissolved in the solution. The autoclave was sealed, warmed up at a speed of 0.5 °C $min^{-1}$ and maintained at 250 °C for 24 h, and was then cooled to room temperature naturally (pH ≈ 3.5). The precipitate was filtered off, washed with 1 N HCl, distilled water and absolute ethanol several times, and then dried in vacuum at 60 °C for 4 h.

X-Ray powder diffraction (XRD) measurements were carried out on a Rigaku D/max-γB X-ray diffractometer with Cu Kα radiation ($\lambda = 1.54178$ Å). Transmission electron microscopy (TEM) images of the samples were obtained from a Hitachi model H800 transmission electron microscope using an accelerating voltage of 200 kV. High-resolution electron microscopy (HRTEM) images, electronic diffraction (ED) patterns and energy dispersive X-ray analysis (EDXA) of the samples that were put onto a copper grid were obtained from a JEOL-2010 transmission electron microscope. Fourier transform infrared (FT-IR) spectra were acquired with a Magna IR-750FT spectrometer in the range of 400–4000 $cm^{-1}$ at room temperature, with the sample in a KBr disk. X-Ray photoelectron spectra (XPS) were recorded on a VGESCALAB MKII X-ray photoelectron spectrometer, using non-monochromated Mg Kα X-ray radiation as the excitation source. Room temperature UV-vis adsorption spectra of the products dispersed in ethanol were recorded using a Shimadzu UV-240 UV/vis spectrophotometer.

## Results and discussion

### Formation and characterization of nitrides

X-Ray diffraction (XRD) patterns reveal the crystalline characteristics and phases of the as-obtained InN [Fig. 1(A)] and AlN [Fig. 1(B)]. All the peaks can be indexed to wurtzite InN (JCPDS card 2-1450, $a = 3.537$ Å, $c = 5.704$ Å) and AlN (JCPDS card 3-1144, $a = 3.113$ Å, $c = 4.981$ Å), respectively.

DOI: 10.1039/b310373k

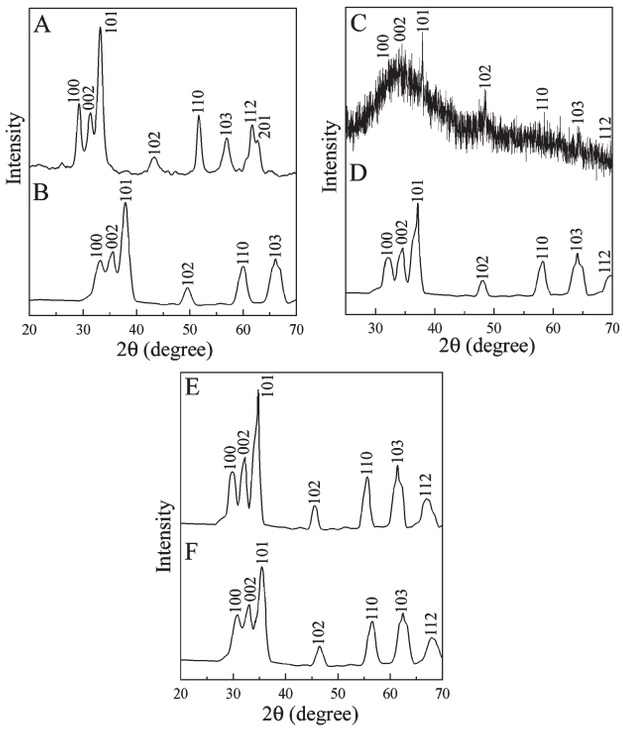


**Fig. 1** XRD patterns of the as-prepared materials: (A) InN, (B) AlN, (C) amorphous GaN before annealing treatment, (D) GaN after annealing treatment, (E) $In_{0.8}Ga_{0.2}N$ and (F) $In_{0.5}Ga_{0.5}N$.

No impurity peaks from elemental In, Al, $In_2O_3$, $Al_2O_3$, $In(OH)_3$, $Al(OH)_3$ or $In_2S_3$, $Al_2S_3$ were found in the experimental range. The XRD pattern [Fig. 1(C)] indicates that GaN is poorly crystalline. The composition of poor-crystalline GaN is also confirmed by the X-ray photoelectron spectrum (XPS) and its crystallinity can be improved by an annealing treatment at 400 °C in $N_2$ with a pressure ranging from $10^{-2}$ to $10^{-3}$ atm for 8 h. Fig. 1(D) shows the XRD pattern of the product after this annealing treatment, in which all the peaks can be indexed to wurtzite GaN (JCPDS card 2-1078, $a = 3.186$ Å, $c = 5.178$ Å). The cell parameters of as-obtained InN, AlN and GaN were determined and are shown in Table 1. Average crystallite sizes estimated by the Scherrer equation are about 19 nm for InN, 16 nm for GaN and 23 nm for AlN. The yields of InN, GaN and AlN are 25%, 20% and 33%, respectively.

Further evidence for the formation of InN, GaN and AlN also can be obtained from the X-ray photoelectron spectra (XPS). In the case of InN, the In core spin-orbit splits into the $3d_{5/2}$ peak at 444.3 eV and $3d_{3/2}$ peak at 451.8 eV [Fig. 2(B)]; the $N_{1s}$ peak [Fig. 2(A), curve 1] can be observed at around 397.5 eV. These results are close to the reported values for bulk InN.[18] As for GaN, the symmetrical gallium Ga 3d peak [Fig. 2(C)] shows the existence of only one signal at 19.3 eV; the $N_{1s}$ peak [Fig. 2(A), curve 2] is at 397.5 eV, which is also close to that of bulk GaN.[18] The Al 2p peak [Fig. 2(D)] at 73.8 eV and the $N_{1s}$ peak at 397.5 eV [Fig. 2(A), curve 3] also confirm the formation of AlN.[18] The

**Table 1** The calculated cell parameters of the as-obtained products

| Phase | $a$/Å | $c$/Å |
|---|---|---|
| InN | $3.532 \pm 0.004$ | $5.706 \pm 0.005$ |
| AlN | $3.110 \pm 0.003$ | $4.985 \pm 0.006$ |
| GaN | $3.188 \pm 0.003$ | $5.175 \pm 0.006$ |
| $In_{0.8}Ga_{0.2}N$ | $3.460 \pm 0.003$ | $5.560 \pm 0.006$ |
| $In_{0.5}Ga_{0.5}N$ | $3.362 \pm 0.002$ | $5.441 \pm 0.006$ |

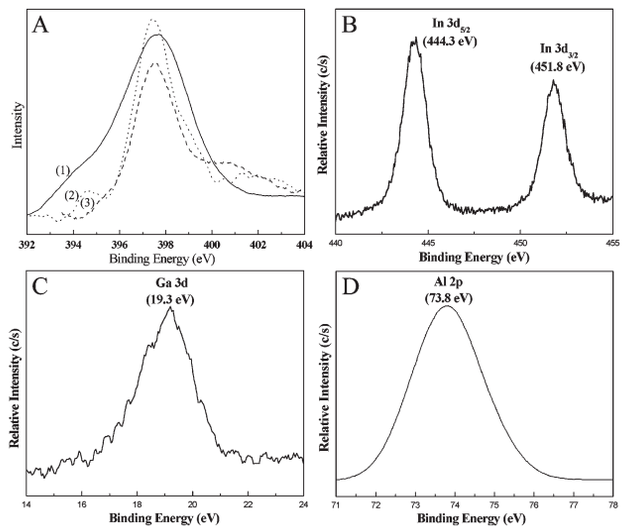


**Fig. 2** XPS spectra of (A) $N_{1s}$ peaks for as-prepared InN (line 1), GaN after annealing treatment (line 2) and AlN (line 3); (B) In 3d peaks for InN, (C) Ga 3d peaks for GaN and (D) Al 2p peaks for AlN.

quantification of peaks gives the ratio of In:N as 1.05:1 in InN, Ga:N as 1.10:1 in GaN and Al:N as 1.08:1 in AlN. The statistical counting deviation in XPS measurements is usually 3–5 at %. No obvious peaks for oxides or other impurities are observed in the XPS spectra. The level of impurities is thus lower than the resolution limit of XPS (1 at %).

To investigate whether N–H bonds exist in the product, the FT-IR spectra of the as-obtained products were recorded. As an example, Fig. 3(A) shows the FT-IR spectrum of as-prepared InN and indicates the absence of NH, $NH_2$ and OH peaks. Thus, the amount of O–H and N–H is below the sensitivity range of IR spectroscopy (0.5%), suggesting a high degree of purity. The FT-IR spectrum shows a broad absorption at *ca.* 510 $cm^{-1}$, assignable to the In–N stretch.[19]

Transmission electron microscopy (TEM, Fig. 4) observation of the samples reveals an average size of about 20 nm for InN, 18 nm for GaN and 25 nm for AlN, which are in good agreement with the XRD results. Fig. 5(A) and 5(B) show high-resolution transmission electron microscopy (HRTEM) images of the obtained InN and GaN nanoparticles, respectively, in which the lattice fringes can clearly be seen and indexed to the (100) and (101) planes of the corresponding phases. The crystalline nature of the products is also confirmed by the selected area electron diffraction (SAED; insets in Fig. 5). The diffraction rings/spots can be indexed as (100), (002), (101), (110), (103), and (112) reflections, according to the hexagonal structure of polycrystalline InN and GaN. The energy dispersive X-ray analyses (EDXA, Fig. 6) give the ratio of In (or Ga) to N in the products (1.03:1), giving compositions of InN and GaN that are in agreement with the XPS results. The statistical counting deviation in EDX measurement is usually 1–2 wt %. The Cu signals are attributed to the Cu grid that the samples are put on. In EDX measurement, all elements heavier than Be can be analyzed with a typical detection limit of 1 wt %. Thus, the content of oxides or other impurities is below 1 wt %.

This synthetic route can also be extended to prepare alloys of group IIIA nitrides. For example, $In_{0.8}Ga_{0.2}N$ and $In_{0.5}Ga_{0.5}N$ have been prepared *via* this route. Fig. 1(E) and 1(F) show their XRD patterns. Interpolated by the Vegard rule from the lattice constants of InN and AlN, the $x$ values in the $In_xAl_{1-x}N$ solid solution coincide with the result of the XPS spectrum. The cell parameters of as-obtained $In_{0.8}Ga_{0.2}N$ and $In_{0.5}Ga_{0.5}N$ were determined and are shown in Table 1.

The optical properties of the as-obtained InN, GaN, AlN, $In_{0.8}Ga_{0.2}N$ and $In_{0.5}Ga_{0.5}N$ nanocrystals were investigated

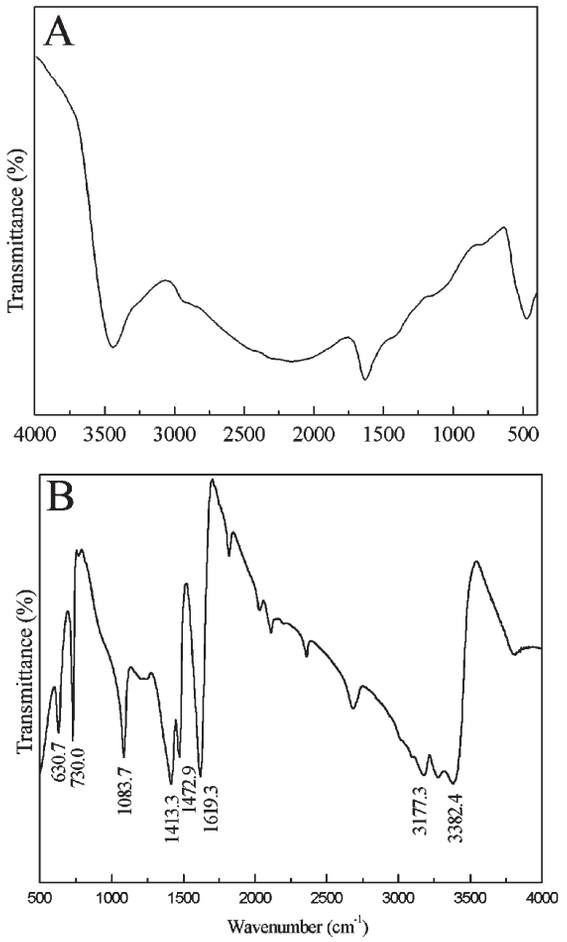


**Fig. 3** FT-IR spectra of (A) as-prepared InN and (B) the solid collected from the solution after reactions.

by UV-vis absorption spectroscopy at room temperature. They (Fig. 7) reveal that the bandgaps of as-prepared InN, $In_{0.8}Ga_{0.2}N$, $In_{0.5}Ga_{0.5}N$, GaN and AlN are 2.1, 2.4, 2.75, 3.6 and 6.3 eV, respectively. This indicates that the bandgaps of group IIIA nitrides and their alloy nanocrystals can cover the region of 2.1–6.3 eV. The blue shifts observed, compared with the corresponding bulk materials,[4] indicate quantum confinement effects in the as-obtained group IIIA nitrides and their alloys nanocrystals.

The solution after completion of the reactions was evaporated and the solid was collected, which was then studied by Fourier transform-infrared (FT-IR) spectroscopy. From the spectrum [Fig. 3(B)], it is found that $(NH_2)_2CS$ is a byproduct of the reactions, since the peaks at 3177–3382, 1413–1619, 1084, 730 and 631 $cm^{-1}$ are indexed to the N–H stretching, N–H bending, N–C–N stretching, C–S stretching and N–H bending vibrations of $(NH_2)_2CS$.[19] Moreover, HCl, HI and $H_2S$ byproducts can also be detected by chemical methods.

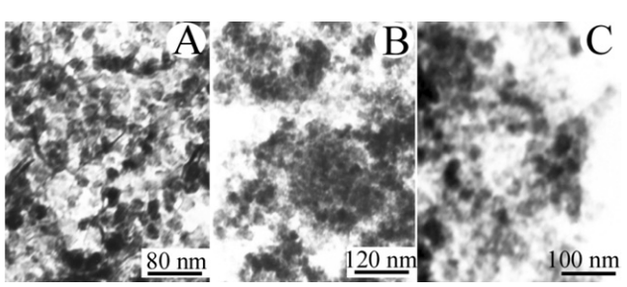


**Fig. 4** TEM images of as-prepared (A) InN, (B) GaN and (C) AlN.

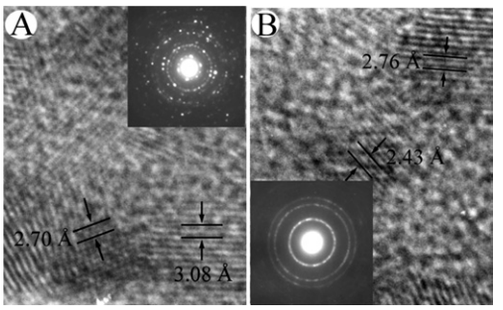


**Fig. 5** HRTEM images and ED patterns of as-prepared (A) InN and (B) GaN after annealing treatment.

The pH value of the solution after reactions is about 3.5. Thus, the overall reaction can be written as follows, based on the above detected products (M = In, Ga, Al):

$$NH_4Cl \rightarrow NH_3 + HCl \quad (I)$$

$$2M_2S_3 + 18NH_3 + 6CS_2 + 3I_2 \rightarrow 4MN + 6(NH_2)_2CS + N_2 + 6HI + 12H_2S \quad (II)$$

It is obvious that the reaction (II) is a key process for the formation of group IIIA nitrides and should include several steps. However, detailed information about each step in reaction (II) is incomplete, since the experimental reactor is sealed and possible intermediate compounds cannot be detected. But a possible mechanism can be proposed, suggested by two known reactions:[20]

$$CS_2 + 2NH_3 \rightarrow NH_4SCN + H_2S \quad (III)$$

$$2NH_4SCN \rightarrow NH:C(NH_2)_2 + NH_3 + CS_2 \quad (IV)$$

Since $(NH_2)_2CS$ is a byproduct of the reactions, it is thought that reaction (V) most probably occurs, leading to the transformation of $NH:C(NH_2)_2$ into $(NH_2)_2CS$:

$$M_2S_3 + 3NH:C(NH_2)_2 \rightarrow M_2(NH)_3 + 3(NH_2)_2CS \quad (V)$$

It was reported that nitrides could be prepared by loss of ammonia from $M_2(NH)_3$ on heating:[20]

$$M_2(NH)_3 \rightarrow 2MN + NH_3 \quad (VI)$$

From the above analysis, the addition of $I_2$ should be indispensible for the formation of nitrides, which has been verified in our experiments. Without adding $I_2$, IIIA nitrides can be

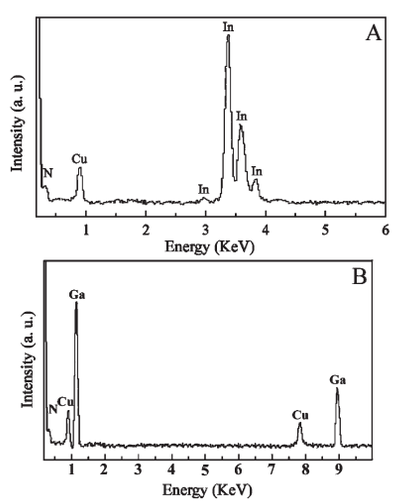


**Fig. 6** EDX of the as-prepared (A) InN and (B) GaN.

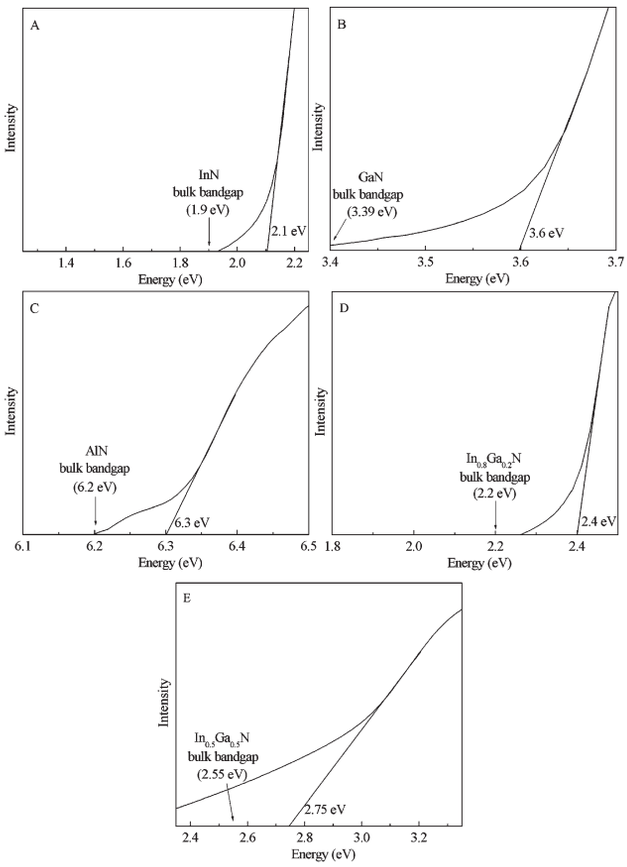


**Fig. 7** UV-vis spectra of as-prepared (A) InN, (B) GaN, (C) AlN, (D) $In_{0.8}Ga_{0.2}N$ and (E) $In_{0.5}Ga_{0.5}N$.

obtained with a yield of *ca.* 5%. While adding $I_2$, the yield of nitrides can be improved to 25%. The role of $I_2$ in the reactions can be described as follows:

$$2M_2(NH)_3 + 3I_2 \rightarrow 4MN + N_2 + 6HI \qquad \text{(VII)}$$

Thus, the above reactions (III), (IV), (V) and (VII) could be possible steps in the overall reaction (II). It is a pity that $NH_4SCN$, $NH{:}C(NH_2)_2$ and $M_2(NH)_3$ are intermediates that cannot be detected by us. Further work is desirable to identify the mechanism of reaction (II).

It is noteworthy that the other reagents are also crucial to the formation of nitrides. (1) $NH_4Cl$ not only provides the nitrogen source, but also makes the reaction system weakly acidic (before reaction pH $\approx$ 6, after reaction pH $\approx$ 3.5), expediting $M_2S_3$ as the group IIIA metal source and preventing group IIIA metal cations from hydrolyzing. Complementary experiments showed that a basic environment is unsuitable for these reactions. If using $NH_3$ (pH $\approx$ 9) as the nitrogen source, oxides rather than nitrides were obtained. (2) Using $M_2S_3$ as the group IIIA metal source not only retards the hydrolysis of the group IIIA metal cations (compared with indium halides), but also provides a group IIIA metal source from a covalent compound, whose polarity is close to that of group IIIA nitrides. With $MX_3$ (X = Cl, Br, I) or their corresponding organometallic compounds as the group IIIA metal source, no group IIIA nitrides can be obtained.

## Conclusions

In summary, the preparation of group IIIA nitride semiconductors in aqueous solution under mild conditions is established for the first time. The reaction was carried out in an aqueous solution with $NH_4Cl$ as nitrogen source at 250 °C. It was found that the bandgaps of IIIA nitrides and their alloy nanocrystals can cover the region of 2.1–6.3 eV. This work opens a new aqueous route to synthesize highly covalent non-molecular solid nitride materials.

## Acknowledgements

This work was supported by the Chinese National Natural Science Foundation, Chinese Ministry of Education and Chinese Academy of Sciences. The authors thank Prof. Shuyuan Zhang for his technical assistance with the HRTEM experiments.

## References

1 (*a*) H. Morkoc and S. N. Mohammad, *Science*, 1995, **267**, 51; (*b*) H. Morkoc, S. Strite, G. B. Gao, M. E. Lin, B. Sverdlov and M. Burns, *J. Appl. Phys.*, 1994, **76**, 1363; (*c*) T. Matsuoka, T. Ohki, T. Ohno and Y. Kawaguchi, *J. Cryst. Growth*, 1994, **138**, 727.
2 D. A. Neumayer and J. G. Ekerdt, *Chem. Mater.*, 1996, **8**, 9.
3 (*a*) S. Nakamura, in *Blue Laser Light Emitting Diodes, [Int. Symp.]*, eds. A. Yoshikawa, K. Kishino, M. Kobayashi and T. Yasuda, IOS Press, Amsterdam, Netherlands, 1996, pp. 119–124; (*b*) F. A. Ponce and D. P. Bour, *Nature (London)*, 1997, **386**, 351.
4 L. M. Sheppard, *Ceram. Bull.*, 1990, **69**, 1801.
5 M. Goano, E. Bellotti, E. Ghillino, C. Garetto, G. Ghione and K. F. Brennan, *J. Appl. Phys.*, 2000, **88**, 6476.
6 R. A. Fischer, A. Miehr, T. Metzger, E. Born, O. Ambacher, H. Angerer and R. Dimitrov, *Chem. Mater.*, 1996, **8**, 1356.
7 M. Boækowski, *Physica B*, 1999, **265**, 1.
8 T. Inushima, T. Shiraishi and V. Y. Davydov, *Solid State Commun.*, 1999, **110**, 491.
9 O. Takai, K. Ikuta and Y. Inoue, *Thin Solid Films*, 1998, **318**, 148.
10 H. Parala, A. Devi, F. Hipler, E. Maile, A. Birkner, H. W. Becker and R. A. Fischer, *J. Cryst. Growth*, 2001, **231**, 68.
11 I. Grzegory, J. Jun, M. Bockowski, S. Krukowski, M. Wróblewski, B. Lucznik and S. Porowski, *J. Phys. Chem. Solids*, 1995, **56**, 639.
12 N. Takahashi, J. Ogasawara and A. Koukitu, *J. Cryst. Growth*, 1997, **172**, 298.
13 (*a*) J. D. Houmes and H.-C. zur Loye, *Chem. Mater.*, 1996, **8**, 2551; (*b*) J. W. Hwang, J. P. Campbell, J. Kozubowski, S. A. Hanson, J. F. Evans and W. L. Gladfelter, *Chem. Mater.*, 1995, **7**, 517.
14 R. W. Cumberland, R. G. Blair, C. H. Wallace, T. K. Reynolds and R. B. Kaner, *J. Phys. Chem. B*, 2001, **105**, 11 922.
15 H. Lu, W. J. Schaff, J. Hwang, H. Wu, G. Koley and L. F. Eastman, *Appl. Phys. Lett.*, 2001, **79**, 1489.
16 (*a*) Y. Xie, Y. Qian, W. Wang, S. Zhang and Y. Zhang, *Science*, 1996, **272**, 1926; (*b*) Y. J. Bai, Z. G. Liu, X. G. Xu, D. L. Cui, X. P. Hao, X. Feng and Q. L. Wang, *J. Cryst. Growth*, 2002, **241**, 189; (*c*) J. P. Xiao, Y. Xie, R. Tang and W. Luo, *Inorg. Chem.*, 2003, **42**, 107.
17 S. Gao, J. Lu, Y. Zhao, N. Chen and Y. Xie, *Chem. Commun.*, 2002, 3064.
18 C. D. Wanger, W. M. Riggs, L. E. Davis, J. F. Moulder and G. E. Muilenberg, *Handbook of X-Ray Photoelectron Spectroscopy*, Perkin-Elmer Corp., Eden Prairie, 1978.
19 K. Nakamoto, *Infrared and Raman of Inorganic and Coordination Compounds*, 3rd edn., Wiley, New York, 1978.
20 (*a*) F. A. Cotton and G. Wilkinson, *Advanced Inorganic Chemistry*, John Wilkey & Sons, Inc., New York, 1972; (*b*) S. C. Chen, C. Y. Tang and Z. D. Ding, *Important Inorganic Reactions*, Shanghai Science and Technology Publisher, Shanghai, 1994 (in Chinese); (*c*) R. K. Singh, B. P. Asthane and H. P. Bisl, *Chem. Phys. Lett.*, 1993, **209**, 390.